PERIODIC ELECTROMAGNETIC FORCES AT ELECTROMAGNETIC MELT STIRRING

A.A. Maksimov[1], M.Yu. Khatsayuk[1], V.N. Timofeev[1]

[1] Polytechnic Institute, Siberian Federal University, Krasnoyarsk, 660074, Russia

Abstract.
The article presents the mathematic modelling of EM-stirrer with due account for the periodic electromagnetic force and free melt surface in the holding furnace. The electromagnetic force effect on the flow generation subject to the free surface was assessed. Findings of the constant and periodic electromagnetic force were benchmarked. Findings of the periodic force effect on the melt flow pattern at different supply frequencies of EM-stirrer and various in-pool melt level were obtained thus providing for the indirect process verification at production site.

Key words: electromagnetic field; free surface; stirring; molten aluminium; computational model; magnetohydrodynamics.

Introduction

The Ural Polytechnic Institute was a good while engaged in development of the electromagnetic stirring for the steel industry [1]. The non-ferrous metallurgy faced the same issues with the increasing demands for multi-component aluminium-based alloys. Circa 1990 this branch is being developed by the Department of Electrotechnology and Electrotechnics of the Polytechnic Institute of the Siberian Federal University jointly with RPC MAGNETIC HYDRODYNAMICS, LLC [2]. Such scientists as I.M. Kirko, L.A. Verte, Yu.M. Gel'fgat and others contributed much in development of the theory of MHD application processes.

Thus, nowadays EM-stirrers are widely used for molten aluminium making in holding furnaces. Such stirrer provides for the wide gap between the melt and the inductor thus increasing the EMF penetration depth with the supply frequency of maximum 1 Hz. Due to such low-frequency impact on the molten aluminium, electromagnetic forces are intermittent. This electromagnetic force creates waves on the melt surface, such waves often providing a basis for assessment of an EM-stirrer performance. Probably the assessment is rough and not always correct. Therewith any existing procedure to measure the in-melt velocity field is strongly limited in commercial furnaces and holding furnaces for aluminium alloys. As such, the EM-stirrer performance is numerically simulated whereat the melt velocity and flow pattern is analyzed.

Earlier articles [3, 4] provide the description and some examples of the EM-stirrer numerical simulation and analysis. Findings of such calculations were

obtained with some assumptions. As regards the complex solution of an electromagnetic problem, one of assumptions is the consistency of the electromagnetic force applied to the molten aluminium:

$$\mathbf{f}_{em} = \text{Re}\{\dot{\boldsymbol{\delta}} \times \overline{\mathbf{B}}\},$$

where $\boldsymbol{\delta}$ is a current density, $\mathbf{B}$ is a field density.

Sometimes the melt flow effect on the electromagnetic field is factored into by introduction of the correction function to the electromagnetic force in order to speed up such calculations:

$$\mathbf{f}_{em} = \left(k_s \cdot \mathbf{f}_\tau; \mathbf{f}_y; \mathbf{f}_n\right);$$

$$k_s = 1 - \frac{v}{2\tau f},$$

where v is a melt velocity, τ is a stirrer pole pitch, f is a frequency, $\mathbf{f}_\tau$ is a tangential force, $\mathbf{f}_y$ is a lateral force and $\mathbf{f}_n$ is a normal force.

Such correction is appropriate only with the comparably low Q-factor of an electric machine when the extreme mechanical performance reaches the deceleration area and becomes close to the linear one within the slip range from 0 to 1. This is characteristic of the low-frequency EM-stirrers of aluminium alloys [5]. In this case it is also evidently assumed that the velocity field in the inductor EMF area is uniform.

Although such correction is quite rough for the process pre-evaluation and identification of the key equipment parameters and operation modes, it is also efficient for the on-line design engineering.

The melt surface waves induced by electromagnetic forces are, as a rule, of no interest and not simulated. Findings of the computational model with the above assumptions allow identifying just the key patterns of electromagnetic stirring.

Development and creation of more detail computational modelling of multi-phase problems, in particular MHD-processes, allows obtaining the more detail results. Ansys Fluent and Maxwell integration is one of such computational modelling procedures.

The main objective hereof is the comparative analysis of the findings of the constant and oscillating EMF calculation. As well as the research of the periodic force effect on the in-furnace melt stirring.

Statement of the Problem.

The "EM-stirrer - furnace bath" system is being considered (Fig. 1-a).

<table>
<tr><td align="center">a)</td><td align="center">b)</td></tr>
</table>
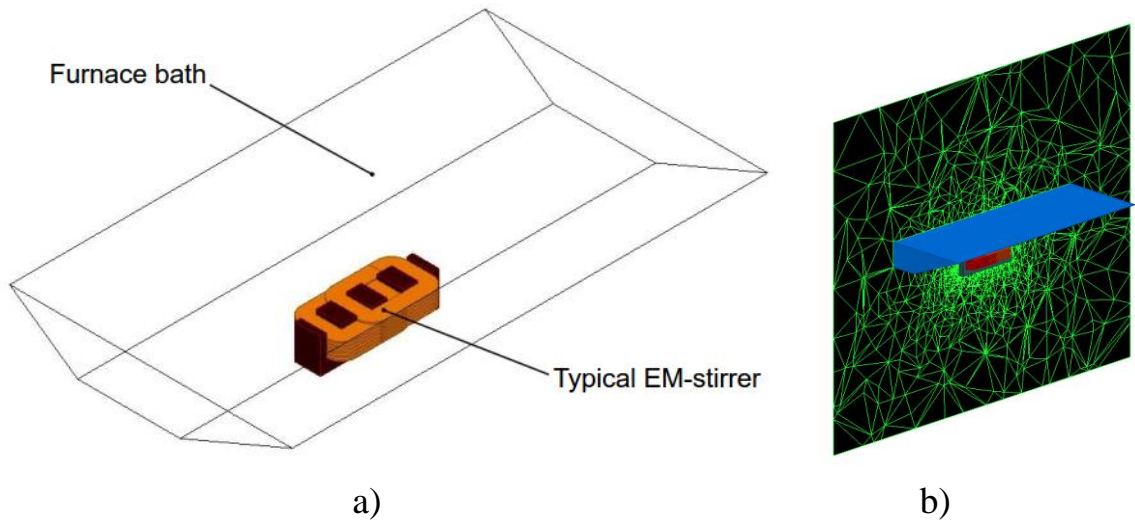
Fig. 1 – Sketch of the system and the computational domain

Dimensions and the key supply parameters of the EM-stirrer as well as the furnace bath dimensions are taken from [4]. Inductor-melt gap is 0.39 m. This inductor is usually powered with AC of 200-400 A and frequency from 0.4 to 1.5 Hz. The total power of the standard-version inductor is 100-140 kVA at the consumed active power of 25-35 kW.

Three in-bath melt levels were considered to review the periodic EMF effect on generation of flows: 0.3; 0.5; 0.9 m (Fig. 2). When the in-bath melt level was 0.5 m, calculations were made with various EM-stirrer frequency. Surface tension of molten aluminium is assumed equal to 0.9 N/m.
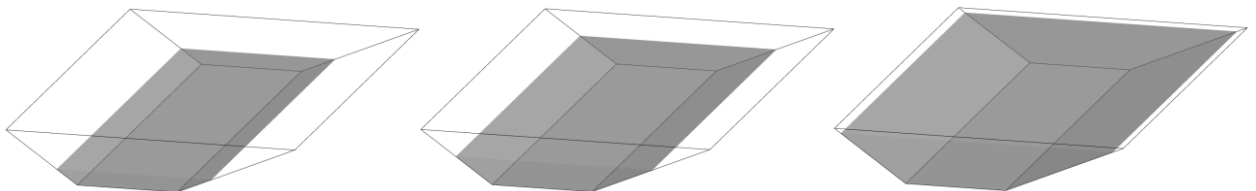
Fig. 2 – Initial melt distribution in the furnace bath in the appropriate pattern.

Computational model.

Multi-phase MHD-problems of the metal stirring are usually solved as two separate problems. One of such solutions is as follows: the stationary electromagnetic force as computed under the EM problem solution is transmitted to CFD (Computational Fluid Dynamics) to solve the hydrodynamic (HD) problem. As an alternative, it is suggested to transfer the complex magnetic vector to the HD solution domain. As for hydrodynamics, MHD module of the Fluent software [6] deals with calculations of electromagnetic force, current density and, finally, of the electromagnetic force (Fig. 3). This module is suitable for the low-frequency calculations which makes it possible to apply for modelling of the EM-stirring.

Solution of the high-frequency problems severely increases the requirements imposed on computational resources because of the time increment decrease.
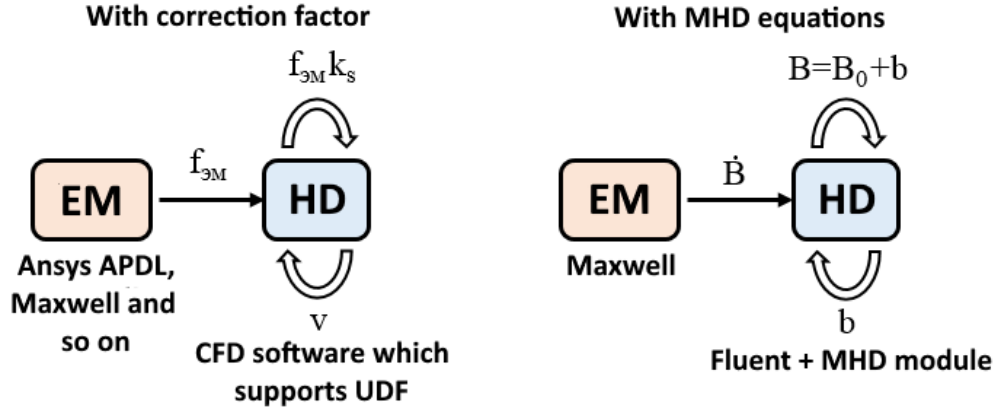
Fig. 3 – Scheme of the two problems' link

A set of equations as applied to MHD-problems consists of the sets of Maxwell equations regardless of the induction current [7]. Equations describing the hydrodynamic processes in electromagnetic field consist of continuity and motion equations [8]. The set of equations shall be completed with VOF model [9, 10] to take into account the free surface, such model consisting of the phase indicator function:

$$\frac{\partial \alpha}{\partial t} + \frac{\partial v_i \alpha}{\partial x_i} = 0$$

$$\alpha = \begin{cases} 1 \text{ cell is filled with phase 1} \\ 0 \text{ cell is filled with phase 2} \\ \quad 0 < \alpha < 1 \text{ interface} \end{cases}$$

The weight function is used to calculate the properties of the liquid in the cell volume:

$$\rho = \alpha \rho_1 + (1 - \alpha)\rho_2$$

$$\mu = \alpha \mu_1 + (1 - \alpha)\mu_2$$

where α is the phase indicator function, ρ is density, μ is kinematic viscosity.

Magnetic field $\mathbf{B}$ in the MHD-problem can be split into the superimposed field $\mathbf{B}_0$ and the induced field $\mathbf{b}$ by the molten metal flow. MHD module shall solve only the induced field $\mathbf{b}$. And field $\mathbf{B}_0$ is solved under the set of Maxwell equations that is the electromagnetic problem.

The induction equation as per the Ohm's law and Maxwell equation will be as follows:

$$\frac{\partial \mathbf{B}}{\partial t} + (\mathbf{v} \cdot \nabla)\mathbf{B} = \frac{1}{\mu\sigma}\nabla^2 \mathbf{B} + (\mathbf{B} \cdot \nabla)\mathbf{v} \tag{1}$$

where μ is magnetic permeability; σ is conduction in a body; $\mathbf{v}$ is the melt velocity vector.

The superimposed field will be:

$$\nabla^2 \mathbf{B}_0 - \mu\sigma' \frac{\partial \mathbf{B}_0}{\partial t} = 0 \tag{2}$$

where σ' is conduction of a medium where the field is generated $\mathbf{B}_0$.

After being rearranged (1-2), the induction equation will be as follows:

$$\frac{\mathbf{b}}{\partial t} + (\mathbf{v} \cdot \nabla)\mathbf{b} = \frac{1}{\mu\sigma}\nabla^2 \mathbf{b} + \left((\mathbf{B}_0 + \mathbf{b}) \cdot \nabla\right)\mathbf{v} - (\mathbf{v} \cdot \nabla)\mathbf{B}_0 \tag{3}$$

and the current density will be calculated by the formula:

$$\mathbf{j} = \frac{1}{\mu}\nabla \times (\mathbf{B}_0 + \mathbf{b}) \tag{4}$$

The Lorentz force is an additional source term for a fluid flow equation, such force being calculated as follows:

$$\mathbf{F}_{em} = \mathbf{j} \times \mathbf{B} \tag{5}$$

Finally, we get a set of hydrodynamic equations for each phase:

$$\nabla\mathbf{v}_i = 0 \tag{6}$$

$$\frac{\partial \alpha\rho_i\mathbf{v}_i}{\partial t} + \nabla(\alpha\rho_i\mathbf{v}_i\,\mathbf{v}_i) + \nabla P = \alpha\rho_i\mathbf{g} + \nabla\alpha\boldsymbol{\tau}_i + \mathbf{F}_s + \mathbf{F}_{em} \tag{7}$$

$$\alpha = \begin{cases} \alpha & \text{phase 1} \\ (1-\alpha) & \text{phase 2} \end{cases}$$

where P is pressure, $\mathbf{g}$ – is a free-fall acceleration vector, $\boldsymbol{\tau}$ is a viscous stress tenser, $\mathbf{F}_s$ is a surface tension force at the interface, $\mathbf{F}_{em}$ – is electromagnetic force. As regards the non-conductive media, there will be no electromagnetic force $\mathbf{F}_{em}$. in the hydrodynamic equation.

This way, both periodic force component and effect of the current density induced by the component flow are being accounted for. Hydrodynamic part of the problem reduces to solution of the specified set of equations in the two-component medium within the in-furnace melt pool (Fig. 1). Boundary conditions at the outer surfaces of the computational domain shall be applied to close the set of equations. Thus, no-slip and impermeability conditions $\mathbf{v} = 0$ shall be applied to the outer boundary of the two-component domain (Fig. 4). The notional phase boundary corresponds to α=0,5 and depends on the initial conditions responsible for the in-furnace melt level in equilibrium, such phase boundary dynamically changing during the calculation. Thereat the outer pool boundary $j_n = 0$ shall be deemed as electrically isolated to solve the MHD problem. Therewith, the superimposed field $\mathbf{B}_0$ is fixed and is set as a matrix of sources obtained from the solved electromagnetic FEM problem [4]. As regards the electromagnetic part of the problem, the total

geometry of the computational domain, inclusive of the non-magnetic part ($\mu = 1$), which boundaries are away from the magnetic field and equal to $B_0 = 0$ (Fig. 1-b) shall be used to determine the field B_0 in the melt. The maximum effective value of the in-melt magnetic field is found at the hearth where the inductor is installed and equals to 0.1 T.

Review of Findings

First, the findings for the continuous and periodic components of the electromagnetic field obtained at 0.4 Hz frequency and 0.5 m melt level with due account of the free surface were compared. The key stirring parameters are the melt velocity, the EM-stirrer is capable of, and the resultant flow pattern.
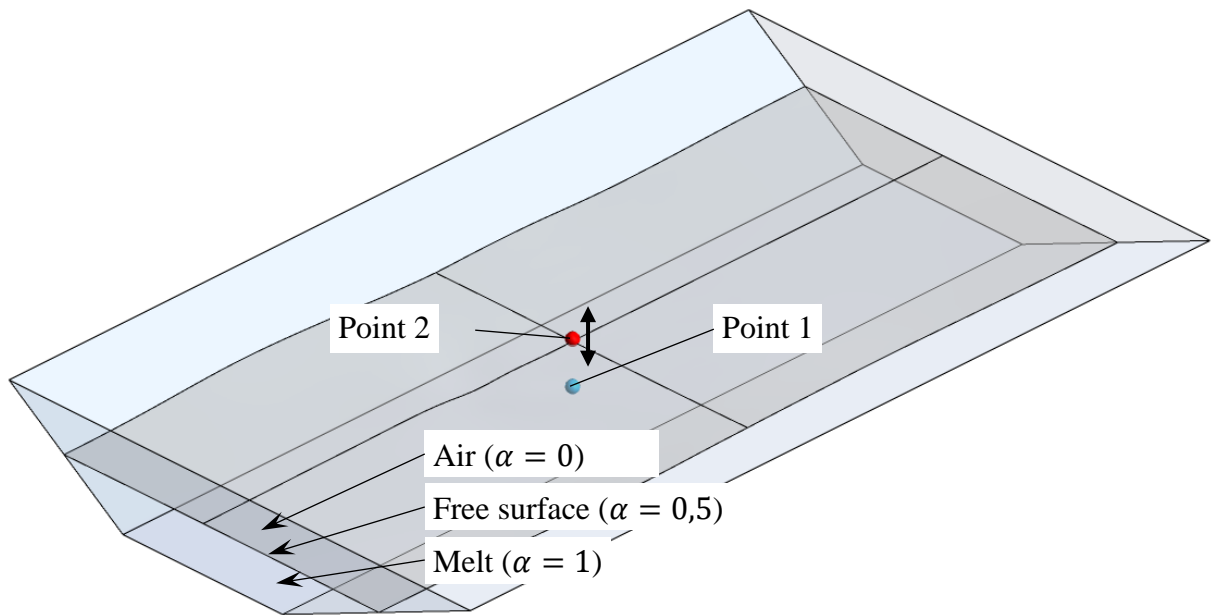
Figure 4 – Typical domains and check points in the furnace bath

The velocity-to-time chart (Fig.5) at Point 1 (Fig.4) was built to compare the various EMFs' effect on the melt.
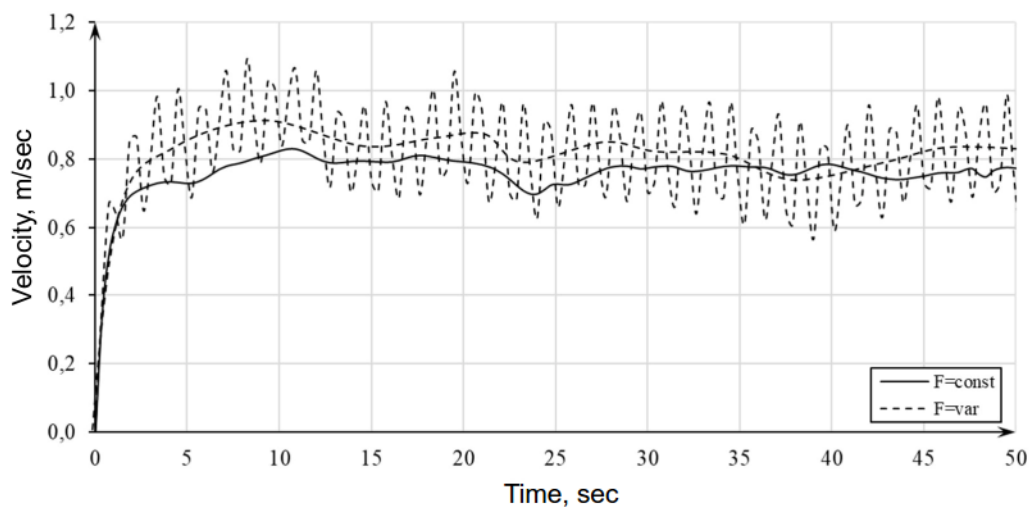
Figure 5 – Metal velocity

It is evident from the chart (Fig. 5) that velocity is periodic when solving the problem with the MHD module. Whereas the EMF-based velocity with the correction factor is constant with some fluctuations due to the flow turbulence. Velocity without regard for the EMF fluctuations is lower than the averaged velocity with fluctuations. The average velocity difference made about 10%. Such difference is attributable to the fact that the actual stirrer electromechanical parameter is not accounted for when solving the hydrodynamical problems with the correction factor.

Figure 6 shows the Point 2 (Fig. 4) comparative graph of the height of the free surface fluctuations depending on the time.
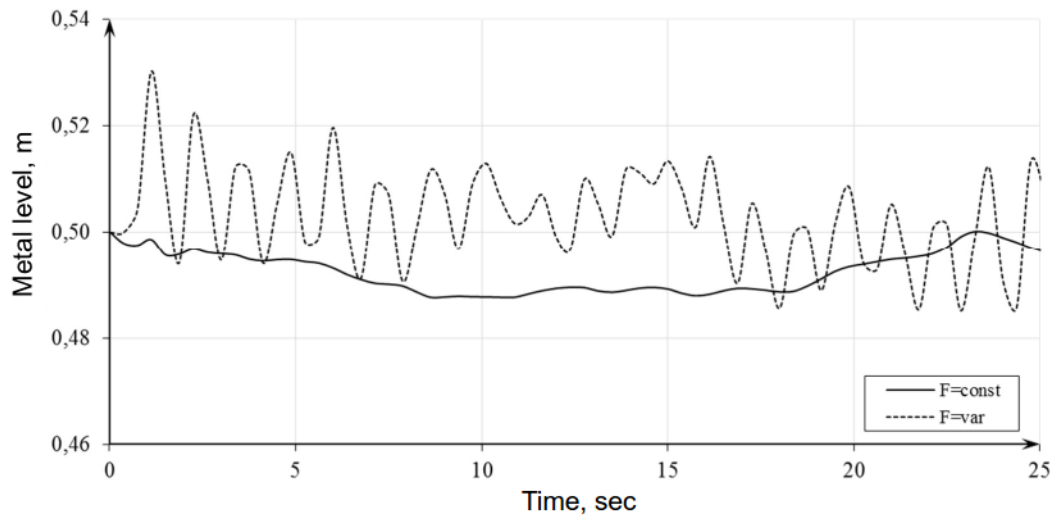
Fig. 6 – Height of the free surface fluctuations

Based on the findings, the free surface fluctuations repeat the velocity fluctuations. Practically no fluctuations are observed with the constant electromagnetic force. Slight surface fluctuations thereat can be attributed to the relevant turbulent velocity fluctuations.

Patterns of the in-pool velocity vector field at different time intervals were obtained to assess the effect of various EMF on the in-melt flow generation (Fig. 7).

Time	MHD module solution	with correction factor

100
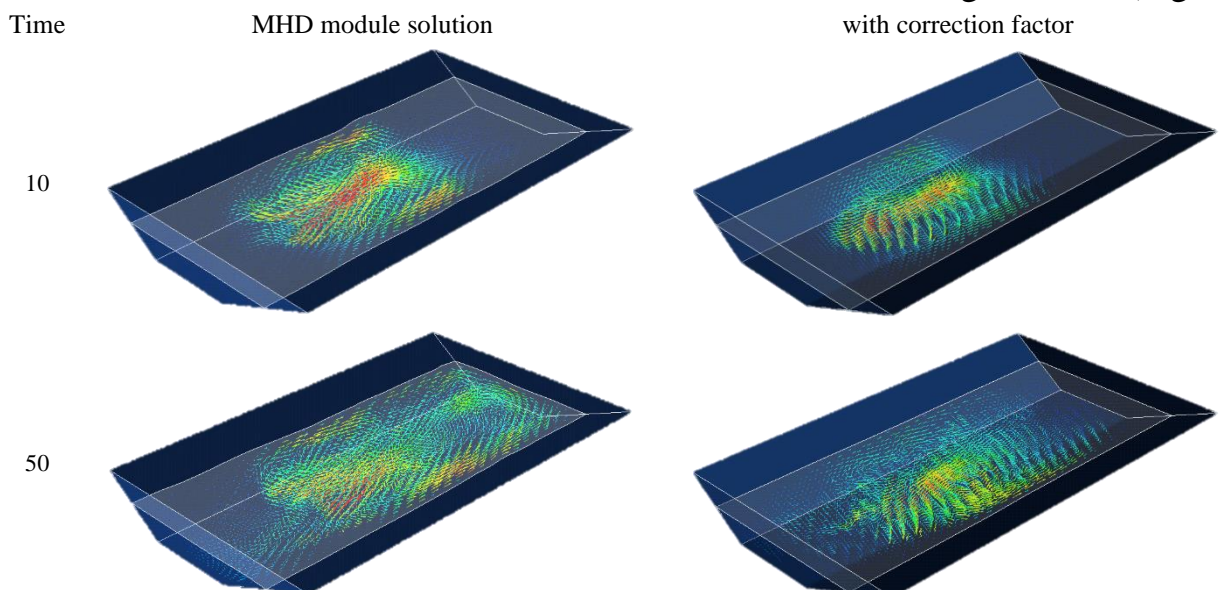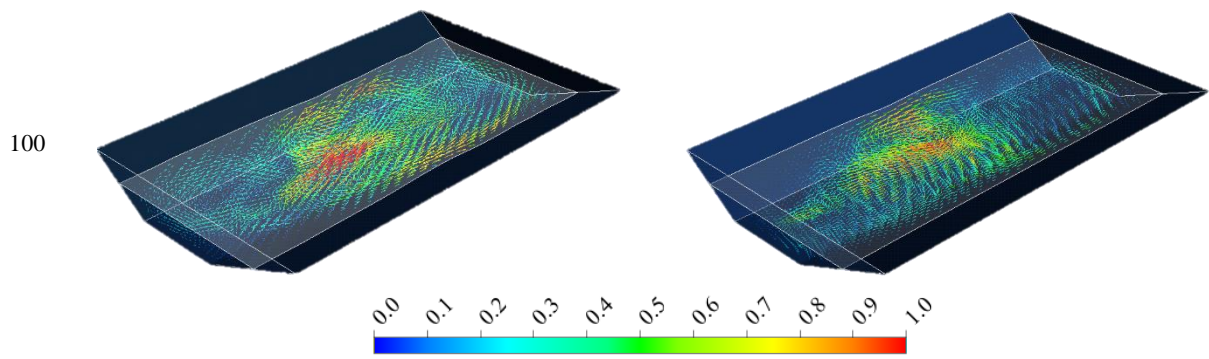
Fig. 7 – In-melt velocity vector field

The effect of the transverse electromagnetic force when applying the MHD module is easy to see on the velocity vector field patterns (Fig. 7). Such force initially creates the counter-flows at lateral edges of the pool. When applying the correction factor, the initial flow was directed towards the tractive force. By the 100 sec. time, patterns of the major flows became identical with the only difference of the average in-pool velocity being lower at the constant force.

Next stage provides comparison of solutions with MHD module at various inductor frequency supply. Time was converted to relative units against the fluctuations' period t´=t/T in order to bring the findings in the graph to the common view. Findings are plotted within the 0 c and 2T time interval.
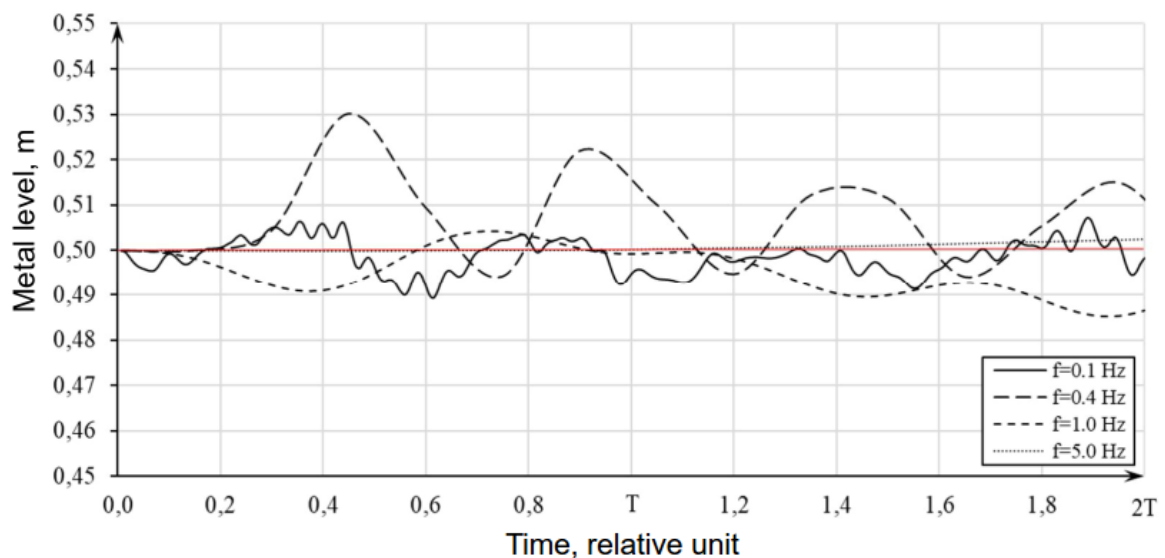
Figure 8 – Metal level at various inductor frequency supply

Figure 8 shows the graph of the height of the melt surface fluctuations to time. Height of the waves being formed on the free surface at 0.4 Hz frequency is higher as compared to other frequency values. One might assume that this frequency is a hydrodynamic resonance. Still, almost no fluctuations are observed when affected by the force at the frequency of f = 5 Hz.
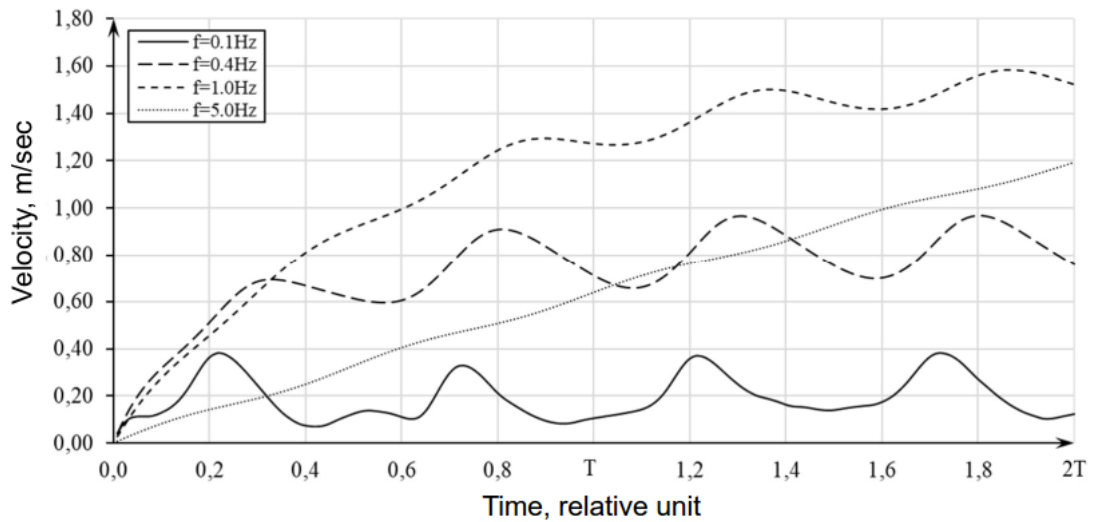
Figure 9 – Melt velocity-to-time at the Point

Velocity analysis (Fig. 9) shows that when the supply frequency is 0.1 Hz, the fluctuations are strongly periodic, almost up to their complete damping, whereas with the 5 Hz supply frequency such fluctuations are not observed. Velocity fluctuations are smoothly damped at the frequencies of 0.4 and 1 Hz respectively. Thus, a regularity can be seen that increase of the supply frequency leads to decrease of the periodic velocity. Time of the velocity change to a steady state made 2-3 secs.

f=0.1 Hz

f=0.4 Hz

f=1.0 Hz

f=5.0 Hz
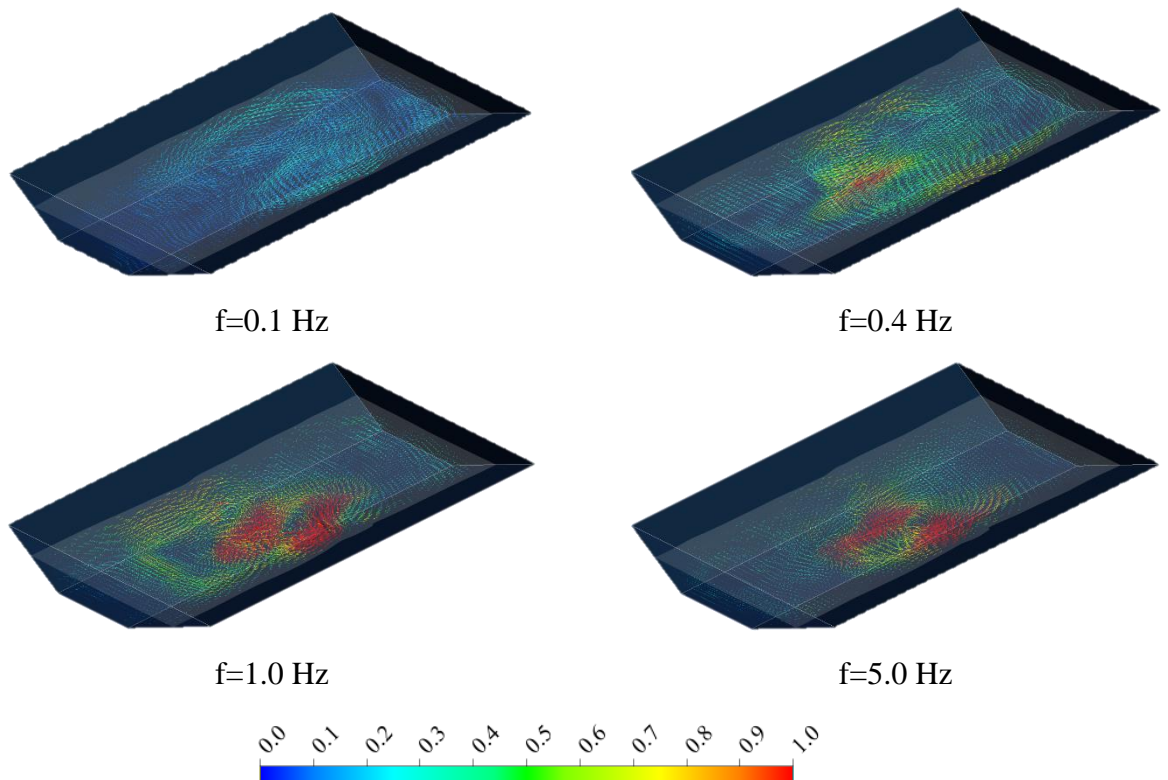
Figure 10 – In-melt pattern of the velocity vector field at the 100 sec. moment of time.

It is obvious from the flow pattern analysis (Fig. 10) that the low-frequency velocity is distributed all along the pool but is of low intensity, thus failing to support

the required stirring performance. Whereas the high-frequency velocity is high but is concentrated over the EM-stirrer area.

Figure 11 shows the velocity vector fields at different in-pool metal levels. Such patterns were obtained at the 2T period of time. The resultant flow patterns showed that the increase of in-pool metal level leads to increase of its velocity and, by the 2T time, the directed melt flow is settled over the high volume of the pool.
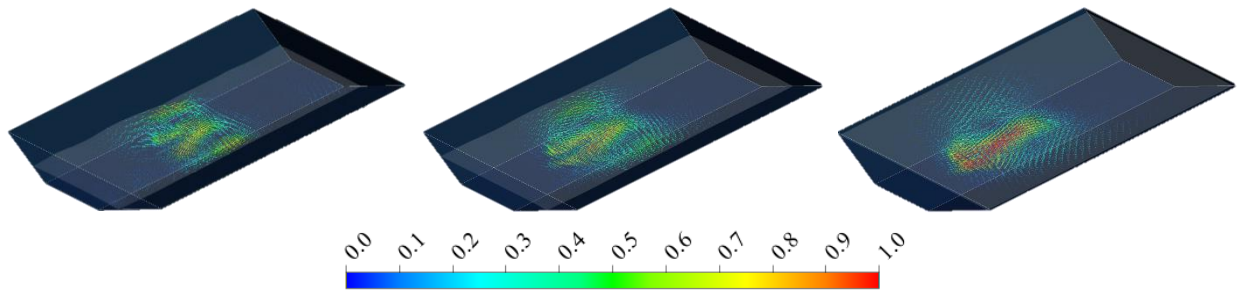
Figure 11 – In-melt pattern of the velocity vector field at different metal level

Conclusion.

This article presents the benchmarks of non-periodic and periodic EM field effect on the melt. Judged by the findings, it may be concluded that, when solving the MHD problem with correction factor which is deliberately inclusive of the slip, the velocity may differ from the actual one because of the electromechanical parameter simplification. Nevertheless, there are slight differences as regards the in-pool flow pattern.

Also, velocity and pattern of flows, as well as the free surface behavior were studied at various inductor supply frequencies and different in-pool metal levels. The findings obtained at that time showed that the higher the inductor supply frequency is, the lower the velocity fluctuations are as well as their performance in the amplitude of the free surface fluctuations. Fluctuations are almost invisible at high frequency values. There is a popular belief that the higher and more intense the free surface fluctuations are, the more effective the stirring is. But the results obtained testify to the opposite. Intense stirring may take place even at the higher frequency values, but the major stirring effect occurs over the EM-stirrer location. As such, relatively high velocity is possible at high frequency which is impossible with low frequency values because of the limited velocity of the travelling magnetic field. It may be concluded from the results obtained that EM-stirrer parameters, especially frequency, shall be selected during the design based on the shape and dimensions of the furnace bath.

Thus, it was found that the periodic electromagnetic force being accounted in a hydrodynamic problem should give the more reliable results. Further researches of the EM-stirrer with various frequency values under this method of solution will help

to find the best supply frequency for furnaces of various geometry and in-furnace melt levels.

References

[1] M. G.Rezin, Advances in electromagnetic stirring of liquid metals, Vol.1, No.2, 130-138, 1965

[2] V. N. Timofeev, M. Y. Khatsayuk, Theoretical design fundamentals for MHD stirrers for molten metals, Vol. 52, No. 4, 495-506, 2016

[3] A.A. Maksimov, M.Yu. Khatsayuk, V.N. Timofeev Comparative assessment of the findings of computational simulation of hydrodynamic processes in the Molten Bath - MHD-stirrer system. *Magazine of the Federal Siberian University. Engineering and Technology, V.11(2018), No2, pp.*138-147

[4] A.A. Maksimov, M.Y. Khatsayuk, V.N. Timoveef. Aspects of Energy Transformation and Energy Control Capabilities in Electric Machines with a Liquid-Metal Working Body. *20th International Conference on Micro/nanotechnologies and Electron Device* (Erlagol, Altai Republic, Russia, 2019), pp.726-730

[5] Baake E., Barglik J., Jakovics A., Khatsayuk M., Lupi S., Nikanorov A., Pavlovs S., Pervukhin M., Timofeyev S., Timofeyev V. MHD technologies in metallurgy. Intensive Course Specific IV. Saint Petersburg: Publishing house of ETU. 2013. 250 p.

[6] Magnetohydrodynamics (MHD). Module Manual. User Guide: FLUENT 6.3 User's Guide. 2006.

[7] A.I. Vol'deck Induction Magnetohydrodynamic Machines with a Liquid-Metal Working Body. L., Energy, 1970. p.272 with a picture.

[8] M. Pervukhin, A. Minakov, N. Sergeev, M. Khatsauk. Mathematic simulation of electromagnetic and thermal-hydrodynamic processes of the system "inductor-ingot" of an electromagnetic mould. Magnetohydrodynamics Vol.47, 2011, No.1, pp. 3-11

[9] Volume of Fluid (VOF) Model Theory. User Guide: FLUENT 6.3 User's Guide. 2006.

[10] Free Surface Flow Simulation Using VOF Method. Mohammed Javad Ketabdari. 2016